Quenches in ϕ^4 theory

Louis Gallouin

Abstract

The work I'm going to talk about here is mainly (and almost exclusively) numerical. Although there is a really rich literature on ϕ^4 theory with a theoretical point of view, that was not the object of my internship and I am not going to detail it. In this report, I'm going to present in the introduction the model I worked on, the context and aim of this study. I'm then going to leave out the generality and talk about what I actually did, meaning describing the program I wrote to achieve our goal, while commenting on the reasons and the means of it's structure. At last, I'll present the few results I obtained, and try to see what is left to be done on this matter. The actual program (coded in python) should be joined to this report, so that the reader can try to run it himself/herself in any way he sees fit. Interesting runs will be commenting throughout the report, to give ideas of parameter choices.

Contents

Acknowledgements

I'd like to thank Leticia Cugliandolo for accepting me at LPTHE during those two months, and for the constant help and support she provided me all through my internship

1 Introduction and exposition of the model

Our work deals with a time-dependent classical scalar field in d spatial dimensions, $\phi(\vec{x}, t)$. We immediately restrict the study to $d = 1$ to reduce the length of computer calculations, though the same study could be carried out in any d. We consider the Hamiltonian

$$H = \int dx \left[\frac{1}{2}(\nabla\phi)^2 + \frac{g}{2}\phi^2 + \frac{\lambda}{4}\phi^4 \right] \tag{1}$$

and the evolution of the field is governed by a "Newtonian" equation of motion

$$m\frac{\partial^2\phi}{\partial t^2} = -\frac{\delta H}{\delta\phi} = \nabla^2\phi - g\phi - \lambda\phi^3 \tag{2}$$

Initial conditions on $\phi(x, 0)$ and $\dot{\phi}(x, 0)$ will be provided.

We start from a Hamiltonian with given values of the coupling constants g_0 and $\lambda_0 = 0$. At time $t = 0$, the field is supposed to be at equilibrium with this Hamiltonian, meaning the initial conditions are distributed along the joint probability distribution :

$$P(\dot{\phi}, \phi) \propto \exp\left[-\beta \int dx \left(\frac{m}{2}\dot{\phi}^2 + \frac{g_0}{2}\phi^2 \right) \right] \tag{3}$$

Here, it just reduces to

$$\begin{aligned} \forall x, P(\phi(x, 0)) &\propto \exp\left(-\frac{\beta g_0}{2} \right) , \\ \forall x, P(\dot{\phi}(x, 0)) &\propto \exp\left(-\frac{\beta m}{2} \right) \end{aligned} \tag{4}$$

which are the "Boltzmann weights".
We then perform an instantaneous quench, meaning we change instantly the couplings constants to *a priori* different g, λ, and we let the field evolve with this new Hamiltonian (following Eq. 2).
Among various questions, we have tried to answer this one : is the field ever going to thermalize, meaning that is the fluctuation-dissipation theorem (FDT) going to be satisfied ? We recall that, if

$$\begin{aligned} R(x, y, t_1, t_2) &= \langle \left(\frac{\delta\phi(x, t_1)}{\delta h(y, t_2)} \right) |_{h=0} \rangle , \\ C(x, y, t_1, t_1) &= \langle \phi(x, t_1)\phi(y, t_2) \rangle \end{aligned} \tag{5}$$

are respectively the linear response function and the two-point correlation function (where h is an external field and $\langle\rangle$ denotes an average over the initial conditions distribution), the FDT states that

$$R(x, y, t_1, t_2) \propto \partial_{t_2} C(x, y, t_1, t_2) \tag{6}$$

Testing this relation numerically will be the aim of our work, as no analytical answer is available. What is however known is that the field should reach a stationary state after a time t_{stat}, but the question remains to know if this is an equilibrium or not.

2 Numerical approach

Let's now go into the core of this internship : the numerical study of this model.

2.1 Numerical modeling, notations

We will consider a 1D chain of length L with periodic boundary conditions $\phi(x,t) = \phi(x+L,t)\ \forall t$. The integration time (time duration of the simulation) will be denoted by T. First we discretise space, with step Dx, and denote $Nx = \frac{L}{Dx}$. We can then subdivide $\phi(x,t)$ into a vector $\vec{\phi}(t) = \big(\phi_1(t), ..., \phi_{Nx}(t)\big)$, where $\phi_i(t) = \phi(iDx, t)$.
Considering these N fields as N classical particles , their Hamiltonian is

$$\begin{aligned} H &= \sum_{i=1}^{Nx} \Big[\frac{m}{2} \dot{\phi_i}^2 + \frac{1}{2} \left(\frac{\phi_{i+1} - \phi_i}{Dx} \right)^2 + \frac{g}{2} {\phi_i}^2 + \frac{\lambda}{4} {\phi_i}^4 \Big] \\ &= T(m\dot{\vec{\phi}}) + V(\vec{\phi}) \end{aligned} \tag{7}$$

with usual classical mechanics notations, where the moment conjugated to ϕ_i is $m\dot{\phi_i}$.
The most important feature that we want to include in our program is the total energy conservation. In the numerical case, the exact conservation is not possible, but we will use high-order symplectic integrators (we will come back to that in a minute) to enforce this condition to the best we can. Indeed, we can expect energy conservation to play a crucial role in the features of the true time evolution, in particular when we have really flat potentials ($\lambda = 0$, and g small), as in those cases the tiniest change in the energy can influence a lot the values taken by the field.
Let's describe in a few words what a symplectic integrator is. Without going into details, it can be shown that (we take one particle for simplicity), if we denote by $q(t)$ the position variable and $p(t)$ the momentum variable, an arbitrary function f(p,q) can be written as :

$$f(p(t), q(t)) = \left(\exp(tL_H) f(p,q)\right)|_{p=p(0), q=q(0)}\,, \tag{8}$$

where $L_H = \{H, \cdot\}$ is an operator taking the Poisson bracket with H. In particular,

$$\begin{aligned} p(t) &= \left(\exp(tL_H) p\right)|_{p=p(0), q=q(0)}\,, \\ q(t) &= \left(\exp(tL_H) q\right)|_{p=p(0), q=q(0)}\,. \end{aligned} \tag{9}$$

Although it is hard in general to find the analytical evolution for p(t), q(t) with a Hamiltonian $H(m\dot{\vec{\phi}}, \vec{\phi}) = T(m\dot{\vec{\phi}}) + V(\vec{\phi})$, it is very easy to do so when we consider $T(m\dot{\vec{\phi}})$ and $V(\vec{\phi})$ separately, thanks to the structure of Hamilton's equations (only one of the two evolves at a time, the other one staying constant). It is then very easy to find the evolution of p(t) and q(t) under L_T, and then under L_V (for example). There is only one problem :

$$\exp(tL_H) \neq \exp(tL_T)\exp(tL_V) = \exp(tL_Z)\,, \tag{10}$$

because of the non-zero commutation relations. The game is to manage to approach H as closely as possible by using successive $\exp(\alpha t L_T)$ and $\exp(\gamma t L_V)$ with some well chosen coefficients. The important point is, with such symplectic integrators we do not evolve approximately our original system, but we evolve EXACTLY a neighbor system. This gives rise to a much better energy conservation compared to "naive" time integrators, as it does not give birth to the usual energy drifts as when evolving the equations.
It's worth noticing that $Z = H + (\textit{polynomial in } t)$; to take Z as close to H as possible, we need to discretise time into timesteps Dt as small as possible, and then evolve those equations step by step. We will denote $Nt = \frac{T}{Dt}$.

We will describe the exact algorithm we used in more details in section 2.3. For now, we just need to remember that we have divided our initial problem into Nx (coupled) evolutions, and will give it proper initial conditions.

2.2 Initial conditions, testing numerical randomness

As we saw in Eq.4, the initial conditions will be chosen randomly and independently for all ϕ_i and $\dot{\phi}_i$. Our goal is, at the end, to measure correlations, averages, ... over this initial probability distribution. It is then important to test the random number generator of the computer, to check that we won't get too much of numerical effects due to the incapacity of a computer to generate pure random numbers. The most crucial point is however that we can't take an average on an infinite number of configurations as it would require an infinite computer time. This "finite size effect" probably is the limiting factor when computing numerical averages.
To test both those effects, we build a really simple program that creates numbers distributed supposedly along a Gaussian distribution $\mathcal{N}(0,1)$ (which is similar to what we will actually use in the main program), and look at their average, variance, and correlations between one another. At the end we see that, for an average over 500 initial conditions, we have differences of 10^{-2} compared to the expected values of what we compute. We will have to keep in mind later when interpreting results the order of magnitude due to those errors.

We build the initial conditions as explained by the discretised Eq. 4

$$\forall i, P(\phi_i(0)) \propto \exp\left(-\frac{\beta g_0}{2}\right) ,$$
$$\forall i, P(\dot{\phi}_i(0)) \propto \exp\left(-\frac{\beta m}{2}\right) , \tag{11}$$

and we obtain $\phi_i(0)$, $\dot{\phi}_i(0)$, as shown for example in Fig. 1.

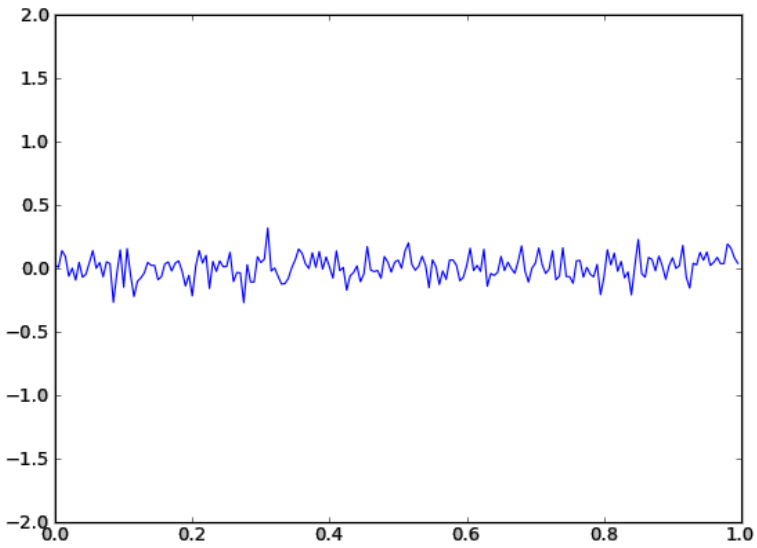

Figure 1: A typical field configuration at $t = 0$, for $\beta g_0 = 100$, $L = 1$.

Let's now discuss in more details the algorithm used to evolve this initial field.

2.3 Temporal evolution

The idea of the symplectic integrators having already been described in section 2.1, let's specify it to our work in this section. At first, at the beginning of the internship, we had begun to work with an order 2 integrator (meaning of the form $\exp(\frac{1}{2}L_V)\exp(L_T)\exp(\frac{1}{2}L_V)$ with the previous notations). We found quite a good energy conservation ($\frac{E-E_0}{E_0} \sim 10^{-5}$, with E the total energy at a given time t, and E_0 the initial total energy), and a quasi-perfect agreement with analytical results when evolving very simple models (like a 0-D harmonic oscillator for example). Nevertheless, and for the reasons we cited previously, we were afraid that this would not be accurate enough in some cases. This is

why we then implemented an even higher-order, of the form

$$\exp(d_1 L_V)\exp(c_2 L_T)\exp(d_2 L_V)\exp(c_3 L_T)\exp(d_2 L_V)\exp(c_2 L_T)\exp(d_1 L_V)\,,$$

where the coefficients are given in Appendix A.
This algorithm has an energy conservation of the order of 10^{-8} to 10^{-9}, and is not so much slower than the previous one. Although we could have wanted once again to get an even better algorithm, we decided arbitrarily to stop here, knowing we could improve it *a posteriori* if we would obtain disturbing results.

By playing with all the parameters of the evolution, we can observe a lot of different behaviors. As expected, the mass parameter controls the "inertia" of the field, and we can observe a changing "speed of evolution" by playing with it. The parameters g and λ control the shape of the potential, position of minima and their depth. When we impose $g < 0$ and $\lambda > 0$, both big enough so that we see the field reaching the new minima in a short time, we observe the formation of kinks, as expected. Due to energy conservation, those kinks are formed and destroyed dynamically. The number of kinks is changing and not at all conserved. We observe, once more as expected, that the less deep the minima are, the fewer kinks exist and the smoother their shape is (the coupling between neighbors becomes relatively stronger). The following figures were built at $\beta = g_0 = 10$ ("not too much noise"), $L = 1$, with various g and λ.

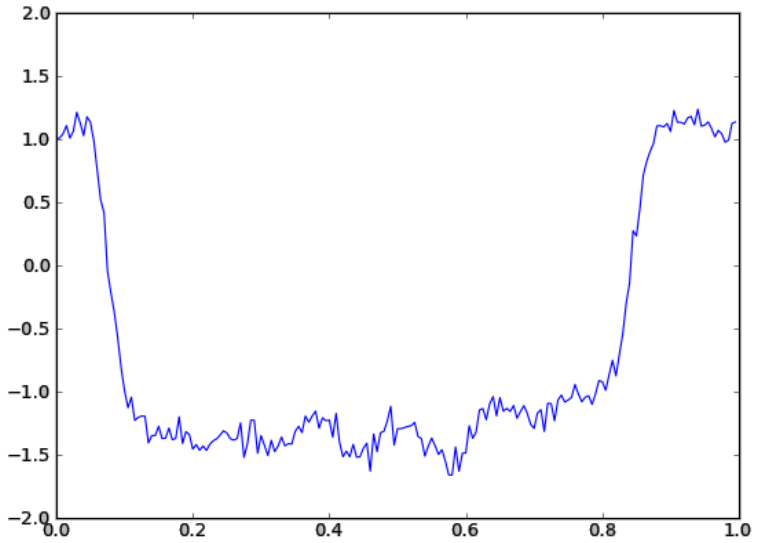

Figure 2: A typical field configuration, for $g = -1000$, $\lambda = 1000$ (deep potential).

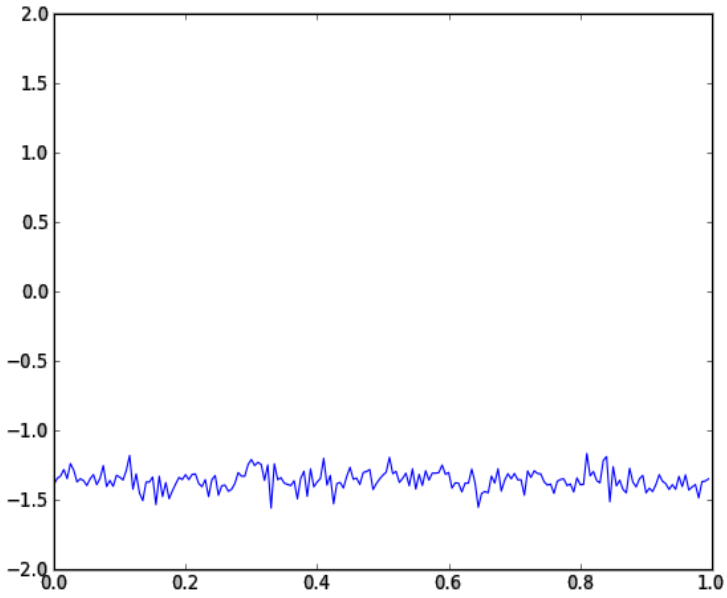

Figure 3: A typical field configuration, for $g = -10$, $\lambda = 10$ (week potential).

Both those figures are of course highly dynamical, and those two are merely recurrent shape that occurs in their respective regime. The reader is encouraged to try out the program if more details are wanted. Regimes where both g and λ are positive gives visually no particular feature.
All in all, the intuitive behavior of the fields is obtained by this algorithm. But we can also test more advance features, like the existence in ϕ^4 theory of solitary waves.

2.4 Testing the validity of the algorithm : solitary waves

Let's now check if our program captures the less intuitive behavior of a ϕ^4 field. It can be shown, and we can verify, that Eq. 2 admits quasi-soliton (solitary wave) solutions when $g < 0,\ \lambda > 0$, meaning that such a solution propagates with no change of shape, but that contrary to actual solitons, collision of two such waves does perturb its form. Such a solitary-wave solution has the form

$$\phi(x,t) = \sqrt{\frac{-g}{\lambda}} \tanh\left[\sqrt{\frac{-g}{2}} \frac{(x - x_0) - cut}{\sqrt{1-u^2}}\right], \tag{12}$$

where $c = \frac{1}{\sqrt{m}}$ is the speed of a free wave in the case $g = \lambda = 0$ (when Eq. 2 reduces to a wave equation), and cu thus is the speed of the solitary wave ($|u| < 1$). The bigger g is at $\frac{g}{\lambda}$ constant, the sharper is the slope (this phenomena was also observed in the previous section).

We can observe such waves (moving or not) with our program by providing adapted initial conditions on ϕ_i, $\dot{\phi}_i$, and changing from periodic boundary conditions to fixed ones.

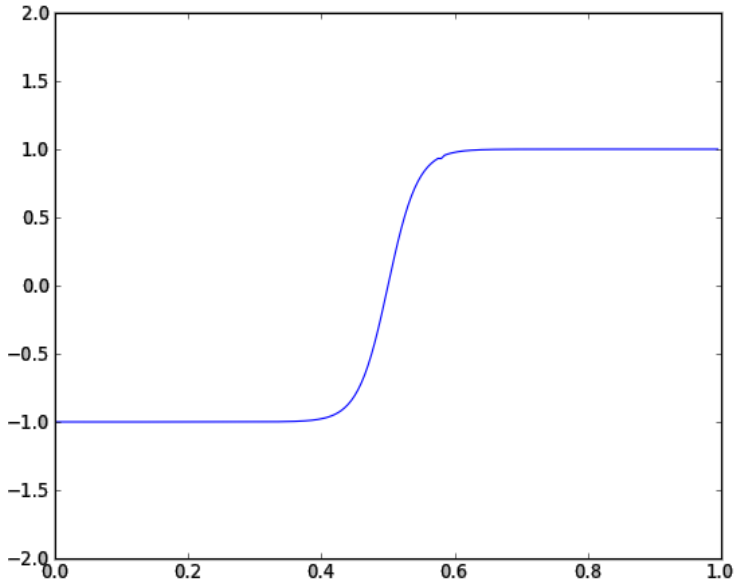

Figure 4: A solitary wave, for $g = -1000$, $\lambda = 1000$.

But we can do more than that. This single solitary wave (let's call it soliton for simplicity) is the only analytic prediction that one can make on ϕ^4 theory about this matter ; but numerically we can observe undeformed kinks (a soliton followed by an anti-soliton) co-moving or not (see Fig. 5) and even really interesting behaviors when a soliton and an anti-soliton collide ! Those behaviors, and particularly the formation of breathers, are really rich and would deserve a more detailed explanation ; nevertheless let's try to sum it up in a few words. When two solitons (soliton and anti-soliton) collide, there are interesting behaviors depending on their relative speed. If it's too high, the solitons go through one another and continue on there initial direction, while being deformed. If it's low enough, the two solitons are bound to one another, and form what is called a breather : they oscillate, going through one another then coming back. It should eventually stop, as some energy is radiated away. And for speeds "not too high, not too low" (for example $u = \pm 0.25$ for the two colliding solitons), we have original behaviors : breather are temporarily formed, and after a few oscillations the waves regain enough energy to go through each other and go to spatial infinity. These are exclusively dynamical behaviors, and that's why I won't show any figures of it. Once more, the reader is encouraged to try out the program to play with those features.

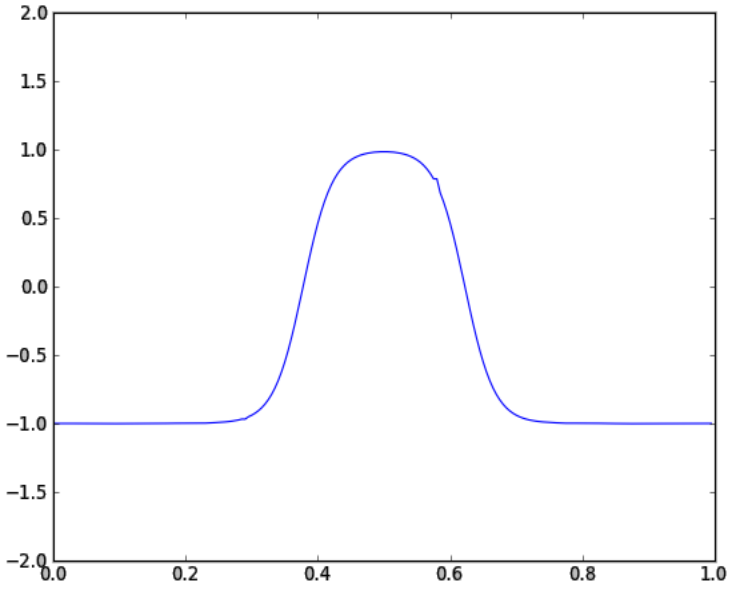

Figure 5: Two solitary waves : a kink ! ($g = -1000$, $\lambda = 1000$).

We can also see, by adding a few noise over a solitary wave, that it is a rather "strong" solution, meaning resilient to perturbations (the shape is globally conserved). This explained the similar shape of the kinks that we observed when starting from pure noise.
All those things, although really interesting by themselves, were only for us tools to check the validity of our program. We are now fairly confident that the program will manage to capture interesting behavior of the field, and we can stop playing with it to begin computing response and correlations functions.

2.5 Computing the correlation and response functions

Let's begin by how computing the response function. If we look at Eq. 5, we see that we have to introduce a perturbative field $h(x,t)$. The perturbed Hamiltonian becomes

$$H = \int dx \left[\frac{1}{2}(\nabla\phi)^2 + \frac{g}{2}\phi^2 + \frac{\lambda}{4}\phi^4 - h\phi \right] \tag{13}$$

When computing the response function, we actually calculate

$$\left(\frac{\left[\phi(x,t_1) \textit{ computed with Hamiltonian } H-(h+\delta h(y,t_2))\phi\right] - \left[\phi(x,t_1) \right.}{\delta h(y,t_2)} \right.$$

$$\left. \frac{\textit{computed with Hamiltonian } H-h\phi\right]}{} \right) |_{h=0} \cdot$$

As we have no way numerically to impose *a posteriori* the condition $h = 0$ (we only get numbers from simulations), we take from the beginning $h = 0$ and we only impose a perturbative field in one point of space and time. From $t = 0$ to t_2, we evolve the field without keeping anything in memory. At t_2, we copy the field and make one evolve with the usual H and the other with $H - \delta h\phi$ during one time step ! We then have to evolve, for every $t > t_2$, 2 fields ϕ and $\phi_{perturbed}$ (with the same Hamiltonian !), and compute at each time step and at each spatial point the difference between those two, divided by the amplitude of the perturbation δh.

The correlation function is more straightforward to compute. Once more week do not compute anything for $t < t_2$. With t_2 and $t_2 + Dt$, we calculate $\frac{\phi(y,t_2+Dt)-\phi(y,t_2)}{Dt}$, and keep it in memory. At each consecutive time-step $t > t_2$, we compute the product of this number with $\phi(x,t)\ \forall x$ (actually $\forall i$ here).

Now, we have to take the averages over the initial conditions : we repeat the whole sequence (choice of initial conditions, evolving the fields and computing at each time-step the two functions) N times (remembering we took N = 500 when testing the initial conditions). This program is the limiting factor, as its runtime is very long.

3 Results and conclusion

Unfortunately, my time at the internship was pretty much up at this point, so I only have a few results to show here. First, we tried for simplicity with N = 50 or 100, but as we could have expected, we found different results from one computation to another, with the same choice of parameters (bad averaging). We then went onto N = 500, and obtained the two functions R,C as functions of x, t_1 for given y, t_2 (with the previous notations). The choice of y can be arbitrary without loss of generality, thanks to translational invariance, but the choice of t_2 may be a bit more subtle. Indeed, we expect (as exposed at the very beginning) the system to reach a stationary sate after a time t_{stat}, and t_2 should be taken $> t_{stat}$ to at least hope to satisfy the FDT. A few results where present for various parameters, but I had taken $t_2 = 0$, the time of the quench (very peculiar, and clearly not at equilibrium). Even with this mistake, we could observe when plotting $R(x,t)$ and $C(x,t)$ at x fixed a "global shape similarity" between the two after quite a long time, which could lead to think

that the FDT may be satisfied.

Those very rough arguments put apart, it is clear that we should run the program with proper choice of t_2 and interpret the results obtained ; this is the next step forecast in this study.

A A few details on the program

The program is written in Python. It plots interactively the evolution of the field, and at the end gives the temporal evolution of the relative difference of energy compared to the initial state. It will ask for the parameters when launched (see sections above for usual parameters). There is one program for each thing discussed earlier (noise → Noise.py, 1 solitary wave → 1Sol.py, 2 solitary waves → 2Sol.py).

Coefficients of the integrator :

$$\begin{aligned} c_2 &= \left(\frac{2^{1/3} + 2^{-1/3} + 2}{3} \right) , \\ c_3 &= 1 - 2c_2 \, , \\ d_1 &= \frac{c_2}{2} \, , \\ d_2 &= \frac{1 - c_2}{2} \, . \end{aligned} \tag{14}$$